35. HYDROTHERMAL EFFECTS ON PROTOKEROGEN OF UNCONSOLIDATED SEDIMENTS FROM GUAYMAS BASIN, GULF OF CALIFORNIA: ELEMENTAL COMPOSITIONS, STABLE CARBON ISOTOPE RATIOS, AND ELECTRON SPIN RESONANCE SPECTRA[1]

Peter D. Jenden, Department of Earth and Space Sciences, University of California, Los Angeles, California
Bernd R. T. Simoneit, Institute of Geophysics and Planetary Physics,
University of California, Los Angeles, California[2]
and
R. P. Philp, Institute of Earth Resources, Fuel Geoscience Unit, CSIRO, North Ryde, 2113 New South Wales, Australia

ABSTRACT

Twenty-seven kerogen samples from the Guaymas Basin were examined to determine the effects of dolerite sill intrusions on recently deposited organic matter. ESR spin density and line width were observed to pass through maxima during the course of alteration. ESR *g* value, however, showed no correlation with maturity. Rather surprisingly, $\delta^{13}C$ decreased by 1 to 1.5‰ in the vicinity of the sills at Sites 477 and 481. In addition, atomic N/C decreased only slightly with proximity to a smaller sill at Site 478. Differences in maturation behavior between Sites 477 and 481 and Site 478 are attributed to dissimilarities in thermal stress and to the chemical and isotopic heterogeneity of Guaymas Basin protokerogen.

INTRODUCTION

The Guaymas Basin is an actively spreading oceanic basin, part of the system of spreading axes and transform faults that extends from the East Pacific Rise to the San Andreas Fault System (Curray et al., 1979). It is therefore tectonically very active and consists of two rift valleys separated by a 20 km transform fault area. The basin is characterized by a high sedimentation rate which keeps its floor and rifts covered while a complex ocean crust and intrusions are forming (Curray et al., 1979).

Site 477 is in the southern rift and Site 481 in the northern rift (the locations of all Leg 64 drill sites are found on the map of the area in the introduction to the shore-based geochemistry). Site 478 is located on the basin floor in the transform fault zone. The sediments recovered were all late Quaternary diatomaceous oozes and turbidites intruded by various sills (Curray et al., 1979).

Site 479 is situated on the Guaymas Slope and consisted primarily of diatomaceous ooze which was laminated below 250 meters sub-bottom (Curray et al., 1979). Site 474 is located at the mouth of the Gulf of California and reflects the influence of open ocean communication in the diatomaceous sediments (Curray et al., 1979).

The sources and characteristics of the organic matter in samples from these sites have been described by Simoneit, Simoneit and Philp, and Galimov and Simoneit (all in this volume, Pt. 2). In this paper, the kerogen[3] isolated by Simoneit and Philp (this volume, Pt. 2) was studied to evaluate further the effects of thermal stress. We discuss the results of electron spin resonance (ESR) spectroscopy, stable carbon isotope analysis, and elemental composition analysis.

EXPERIMENTAL METHODS

Twenty-seven kerogen samples from Sites 474, 478, 479, and 481 were analyzed. The kerogen isolation procedure is described in Simoneit and Philp (this volume, Pt. 2). No attempt was made to remove humic and fulvic acids.

For ESR analysis, the kerogens were sealed under vacuum in 4 × 3 mm quartz tubes and scanned using a Varian E-12 spectrometer. The spectra were recorded at a microwave frequency of 9.5 GHz and a power output of 2 mW. The magnetic field was modulated at 100 kHz frequency and 5 gauss amplitude, and absorption occurred around 3380 gauss. The line width, ΔH, was measured between extrema of the first derivative absorption spectrum. Varian strong pitch standard (0.1% in KCl) was used to calibrate *g* value and spin concentration measurements. To calculate *g* value the following formula was used:

$$g_{\text{sample}} = g_{\text{standard}} \left[\frac{H \text{ standard}}{H \text{ sample}}\right],$$

where *H* refers to the magnetic field strength at maximum resonance. Spin concentration, *N*, was assumed to be proportional to the first derivative absorption intensity, *I*, times the line width, ΔH, squared:

$$N \propto I\,(\Delta H)^2.$$

Values were normalized to % carbon in the kerogens.

For carbon isotope analysis, 10-mg samples of kerogen were combusted at 850°C in 7 × 9 mm quartz tubes in the presence of CuO wire and Ag foil (Frazer, 1962). Carbon dioxide was isolated, measured, and collected on a vacuum line for analysis using a Varian MAT 250 stable isotope mass spectrometer. The kerogens were found to average only 10–15% carbon, so that further purification was required to prevent erroneous H/C determinations (Durand and Monin, 1980). Digestion for 24 hr. in an aqueous solution of 25% $AlCl_3 \cdot 6H_2O$ dissolved large amounts of fluoride minerals precipitated during HF treatment. After water washing and lyophilization, macroscopic pyrite was removed from samples taken from Cores 477-22, 477A-5, 477A-9, 478-13 and 478-40, and from Sections 478-29-1 and 478-29-2 (slick) by

---

[1] Curray, J. R., Moore, D. G, et al., *Init. Repts. DSDP*, 64: Washington (U.S. Govt. Printing Office).

[2] Present address: School of Oceanography, Oregon State University, Corvallis, Oregon.

[3] "Kerogen" usually refers to insoluble, diagenetically altered organic matter found in lithified sediments. In this paper, however, the term "kerogen" is used in a general sense to refer to insoluble organic matter regardless of the degree of thermal alteration or the extent of sediment lithification. "Protokerogen," as used, strictly refers to highly immature kerogen containing appreciable concentrations of biopolymers susceptible to biological degradation (Stuermer et al., 1978).

density separation in $CBrCl_3$ (specific gravity ~2). The heavy liquid was removed by cutting and rinsing with hexane and the kerogen was dried under a stream of nitrogen gas. These procedures raised the average carbon content in the kerogen to approximately 40%. Samples from Site 477 and Section 481-11-2 were sent to the Microanalytical Laboratories at the University of California, Berkeley, for carbon, hydrogen, and nitrogen determination. The remaining samples were analyzed at UCLA according to the methods outlined in Frazer (1962) and Peters (1978).

RESULTS

ESR data, carbon isotope composition, atomic H/C and N/C ratios, and %C of the kerogen after aluminum chloride digestion are recorded in Table 1. The narrow range in carbon isotope composition of the kerogens, which averages −21‰, is characteristic of marine organic matter (Degens, 1969). The same carbon isotope composition (~ −21‰) was also observed for unaltered surface sediments from the northern rift of the Guaymas Basin (Site 30G; Simoneit et al., 1979). Immature kerogen samples show H/C ratios varying between 1.0 and 1.2 and N/C ratios between 0.045 and 0.065. These parameters decline to values as low as 0.4 and 0.02, respectively, near contacts with the dolerite intrusions. ESR spin concentrations vary between $1\text{–}10 \times 10^{17}$ spins/per gram carbon (g C) for immature kerogens and 200×10^{17} spins/g C for the highly altered kerogens at Site 481. ESR line width values show considerable scatter between ~4 and 6.5 gauss for kerogens of intermediate maturity. An exception is the highly altered kerogen from Section 477A-9-1, which shows a line width of 7.7 gauss. This kerogen also shows the lowest H/C ratios (0.011) and the lowest $\delta^{13}C$ value (−23.5‰). The g values of all but one kerogen sample lie between 2.0027 and 2.0031.

Figures 1 to 3 show H/C, $\delta^{13}C$, N, and ΔH plotted against depth for Sites 477, 478, and 481. Data from Holes 477 and 477A are combined in Figure 1. The base

Table 1. Analytical data for kerogen samples from the Gulf of California.

No.	Sample (interval in cm)	Sub-bottom Depth (m)[a]	Elemental Analysis: %C[b]	Elemental Analysis: Atomic H/C	Elemental Analysis: Atomic N/C	$\delta^{13}C$[c] (‰)	ESR Analysis: N ($\times 10^{17}$ spins/g C)	ESR Analysis: Line Width (gauss)	ESR Analysis: g
1	474-6-5, 32–34	46.3 (46.8)	30.8	0.98	0.051	−20.9	1.5	4.6	2.0028
2	477-5-1, 81–91, 94–96	30.4 (36.7)	43.9	1.18	0.060	−20.7	1.1	4.2	2.0027
3	477-5,CC	32.6 (39.0)	47.6	1.06	0.049	−20.8	2.4	4.1	2.0030
4	477-7-1, 124–126	49.7 (56.8)	28.9	0.94	0.045	−20.8	34	5.1	2.0030
5	477-7-2, 14–16	50.1 (57.2)	25.1	0.42	0.037	−22.4	120	5.1	2.0028
6	477-17-3, 44–46	127.9 (133.4)	34.6	0.61	0.027	−21.7	98	4.7	2.0029
7	477-20-2, 61–63	155.1 (161.8)	36.3	0.51	0.024	−21.2	140	4.2	2.0028
8	477-22-1, 26–28	172.3 (179.3)	41.9	1.12	0.047	−20.4	11	4.4	2.0024
9	477-23-1, "slick"	185.0 ±0.7	19.9	0.80	0.013	−21.4	n.d.[d]	n.d.[d]	n.d.[d]
10	477A-5-1, 44–46	191.4 (199.6)	41.8	0.62	0.019	−22.7	27	5.6	2.0028
11	477A-9-1, 39–41	229.4 (237.6)	67.1	0.45	0.011	−23.5	61	7.7	2.0030
12	478-2-2,3,6; 478-3-1, composited	8.0 to 13.2	42.9	1.05	0.063	−21.1	3.4	4.0	2.0028
13	478-13-1,2, 138–140, 116–118	110.0 (114.0)	44.4	0.89	0.038	−20.7	42	4.1	2.0028
14	478-29-1, 57–59 124–126	251.4 (254.4)	46.8	0.95	0.048	−20.8	25	5.9	2.0030
15	478-29-2, 108–110	253.1 (255.9)	32.2	0.50	0.045	−20.2	56	6.1	2.0028
16	478-29-2, 129–131	253.3 (256.5)	41.4	0.53	0.037	−20.6	9.2	5.2	2.0029
17	478-29-2, "slick"	252.7 ±0.7	59.3	0.64	0.045	−20.9	85	6.4	2.0028
18	478-30-1, "slick"	257.6 ±0.7	50.1	0.49	0.052	−20.6	17	5.3	2.0031
19	478-40-2, 61–63	338.1 (343.3)	55.0	0.45	0.031	−20.9	45	4.5	2.0027
20	479-29-5, 114–116	266.6 (266.6)	34.4	1.20	0.046	−19.7	1.5	4.2	2.0028
21	481-11-2, 140–145, wood	50.4 (50.6)	39.0	1.38	0.022	−25.1	n.d.[d]	n.d.[d]	n.d.[d]
22	481A-12-1, 107–109	147.6 (148.8)	27.4	0.87	0.041	−21.1	14	5.1	2.0028
23	481A-14-3, 50–52	169.0 (172.5)	47.8	0.49	0.023	−21.9	170	4.2	2.0030
24	481A-14-4, 2–4 cm	170.0 (173.5)	52.0	0.46	0.021	−21.9	200	4.2	2.0027
25	481A-14-4, 52–54	170.5 (174.0)	51.7	0.49	0.021	−22.0	180	4.1	2.0027
26	481A-18-1, 27–29	203.8 (212.4)	33.2	0.84	0.037	−21.7	65	5.8	2.0028
27	481A-20-1, 60–62	223.1 (230.4)	39.9	0.98	0.050	−21.0	5.1	5.2	2.0031

[a] The sub-bottom depth is given according to the DSDP convention and (in parentheses) as it is calculated upward from the core catcher.
[b] Determined after aluminum trichloride digestion and, in some cases, heavy liquid separation.
[c] Stable carbon isotope composition recorded in parts per thousand deviation from the PDB Chicago standard.
[d] Not determined because of insufficient material.

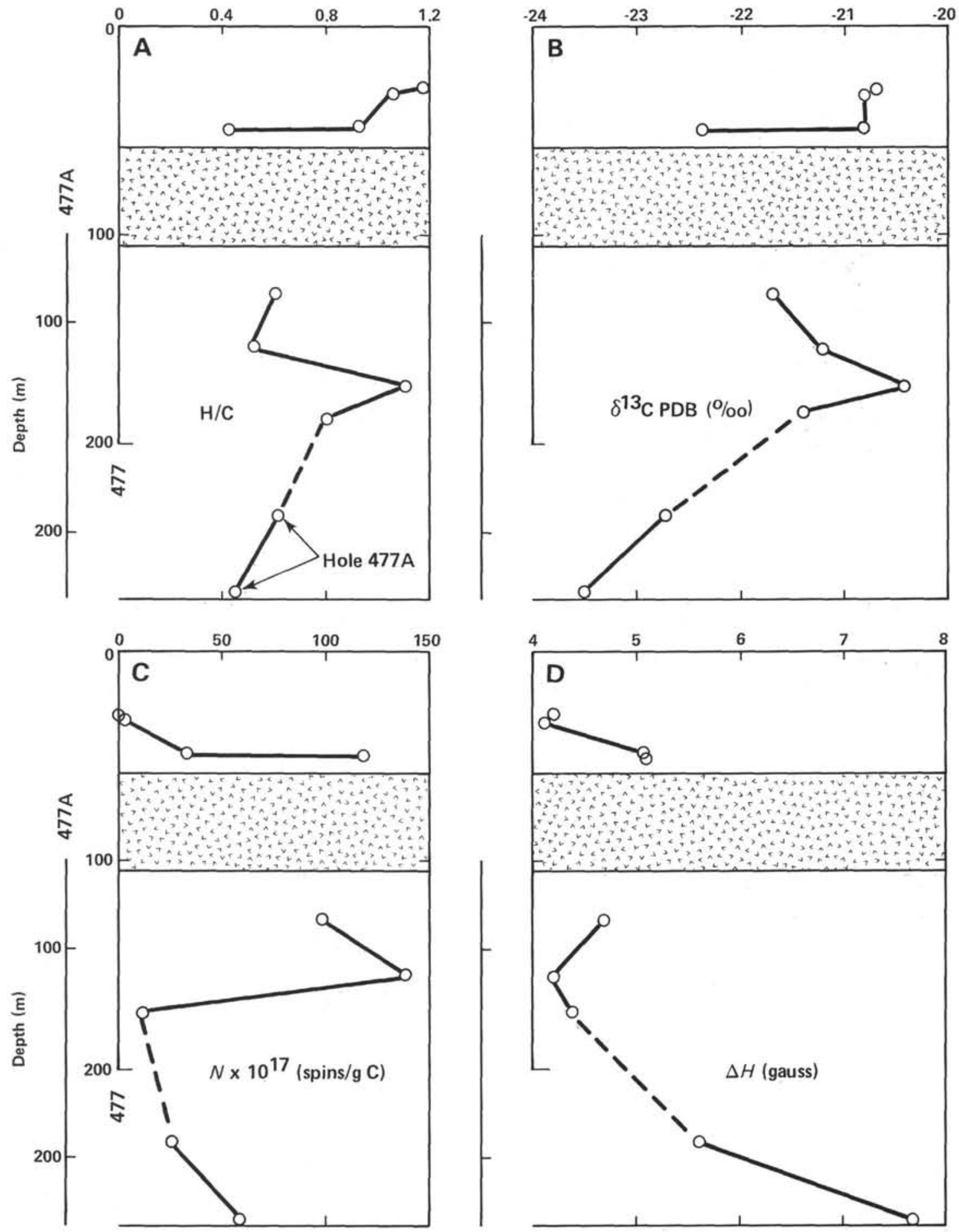

Figure 1. Plots of (A) atomic H/C, (B) $\delta^{13}C$, (C) ESR spin density (N), and (D) ESR line width (ΔH) versus depth for kerogen samples from Holes 477 and 477A. The base of the dolerite sill is used as a common reference point for plotting the data. Note the slight offset between the two depth scales. The points from Hole 477A are connected to those from Hole 477 by a dashed line to indicate trends.

of the dolerite sill is used as a common reference point, and since the sill was encountered 30–40 meters lower in the sedimentary column in Hole 477 than in Hole 477A, the depth scales for the two holes are offset. Depth assignments for all the holes are uncertain because of poor core recovery and may vary by up to 9.5 meters. Minimum depth (adopted by DSDP convention and plotted here) and maximum depth are recorded for each sample in Table 1.

All four parameters in Figures 1–3 show the thermal influence of the dolerite intrusions. In addition, the profiles in Figure 1 indicate a deeper heat source at Site 477.

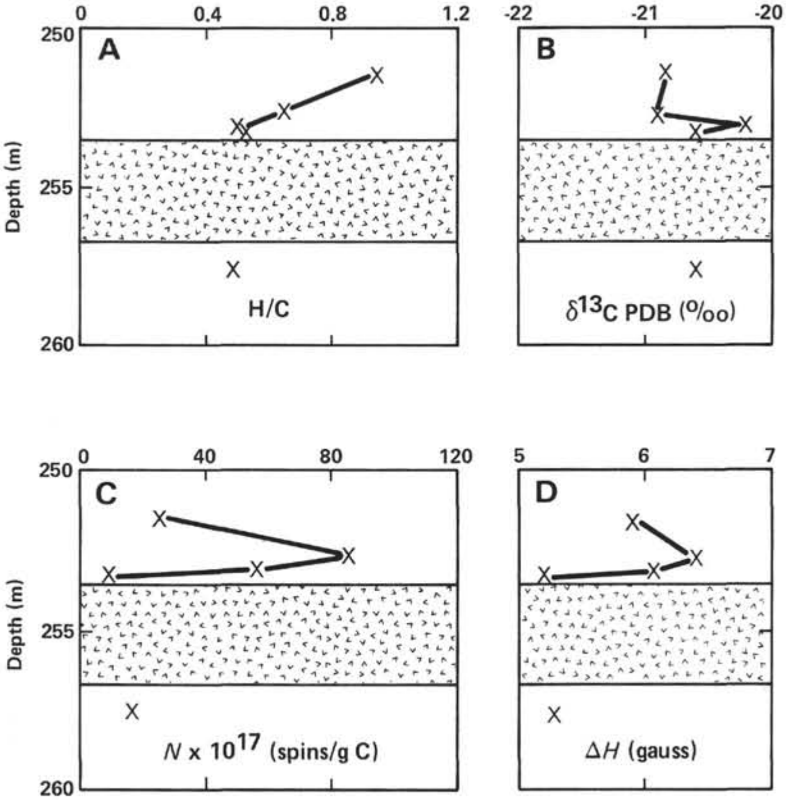

Figure 2. Plots of (A) atomic H/C, (B) $\delta^{13}C$, (C) ESR spin density (N), and (D) ESR line width (ΔH) versus depth for selected kerogen samples from Site 478.

DISCUSSION

Elemental Composition Data

The kerogen H/C diminishes at all three sites as the sills are approached (Figs. 1A–3A). This is due to the thermal generation of water, of methane and light hydrocarbons (Galimov et al., this volume, Pt. 2), and of C_{15}^{+} bitumen (Simoneit and Philp, this volume, Pt. 2). Concurrent with the loss of hydrogen-rich volatiles is a loss of nitrogen, probably as ammonia, which is reflected in the N/C ratios. N/C is plotted against H/C in Figure 4 and clearly decreases with increasing kerogen maturity. Nevertheless, nitrogen seems to be released more readily at Sites 477 and 481 (arrowed path) than at Site 478, where almost all the points show higher nitrogen concentrations for equivalent H/C ratios.

Section 477A-9-1 has the lowest N/C ratio of all the samples (0.11). It also has the lowest $\delta^{13}C$ value (−23.5‰) and greatest ESR line width (7.7 gauss). These data might be explained by the presence of pyrobitumen, which typically has low N/C values. Waples (1977) determined a median N/C ratio of 0.009 for a suite of 92 solidified bitumens. Pyrobitumen might also be expected to be isotopically light, since bitumen is often 1‰ or more depleted in ^{13}C relative to its parent kerogen (Welte et al., 1975).

Simoneit et al. (1981) studied the thermal alteration of kerogen in Cretaceous black shales by diabase sill intrusions in the Eastern Atlantic (DSDP Site 368). For kerogen adjacent to the sills, they found N/C ratios clustering between 0.007 and 0.027. These values are consistent with those measured in the present study for Sites 477 and 481 but are lower than the 0.03–0.05 range for the highly altered kerogen from Site 478.

Why are the N/C ratios of kerogen from Site 478 so high? Since Sites 477, 478, and 481 are all located in the Guaymas Basin within 20 km of one another, extreme compositional differences between protokerogens from these sites do not seem likely. Simoneit and Philp (this volume, Pt. 2) note striking similarities between pyrograms of protokerogens from the three sites and suggest a common, autochthonous microbial origin. The differences in N/C ratios are more likely related to sill thickness and, consequently, time of heating. Four of the five samples from Site 478 with high N/C ratios were located within two meters of the very thin (3.2 m) sill shown in Figure 2. The samples from Sites 477 and 481 were, in contrast, recovered near sills ten times as thick. The high N/C ratios at Site 478 may therefore result from less intense thermal stress and weaker hydrothermal convection. Less intense thermal stress at Site 478 might have preserved a larger proportion of refractory cyclic or aromatic nitrogen and, without strong hydrothermal convection to remove cracking products, it is possible that some nitrogen has been reincorporated into the kerogen structure.

Stable Carbon Isotope Data

The maturation behavior of $\delta^{13}C$ also differs from Sites 477 and 481 to Site 478. Figures 1B and 3B show that in the vicinity of the dolerite sills at Sites 477 and 481, $\delta^{13}C$ decreases by 1–1.5‰ relative to unaltered pro-

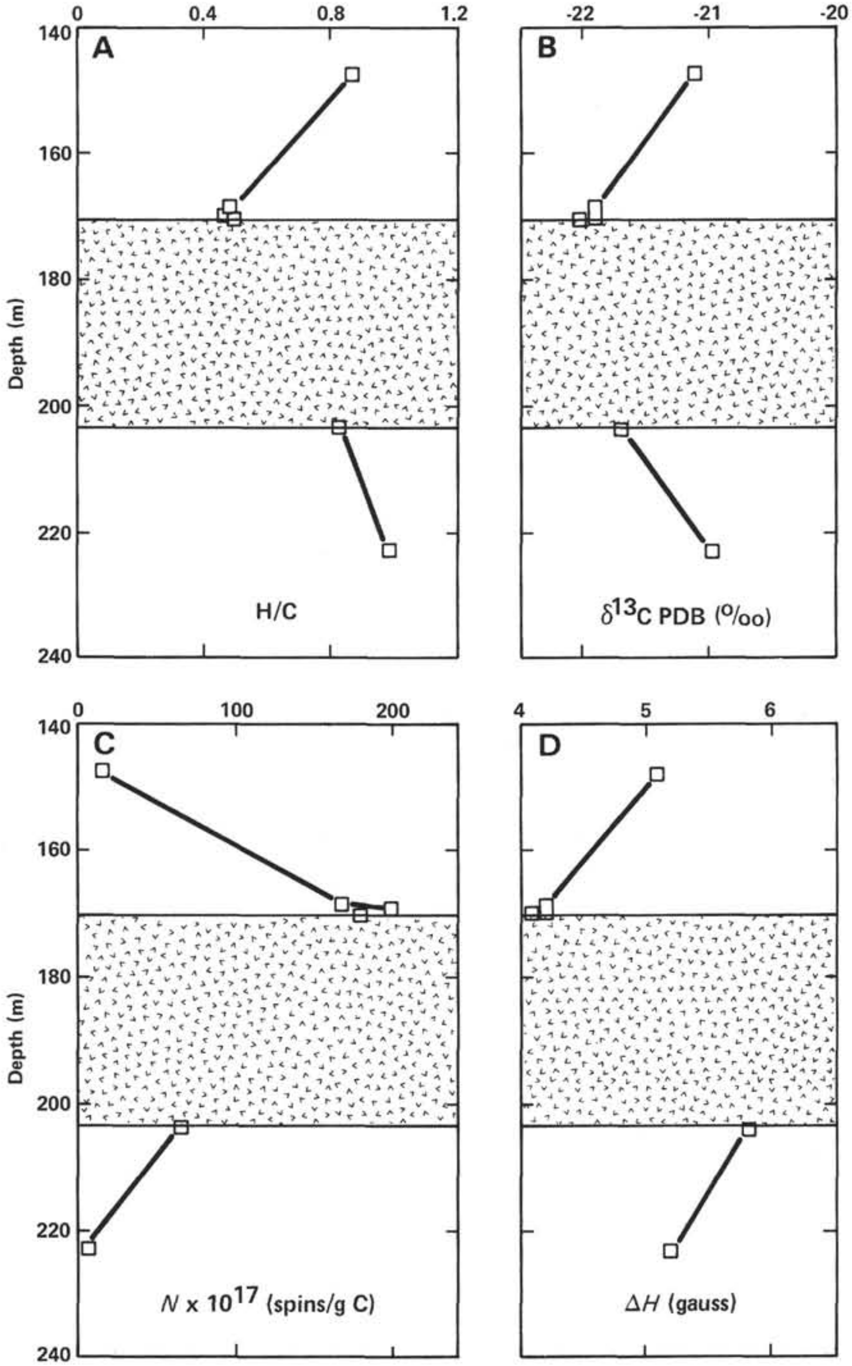

Figure 3. Plots of (A) atomic H/C, (B) $\delta^{13}C$, (C) ESR spin density (N), and (D) ESR line width (ΔH) versus depth for kerogen samples from Hole 481A.

tokerogen. In contrast, Figure 2B shows that kerogen near the small sill at Site 478 preserves roughly the same isotopic composition as its immature progenitor. Figure 5 is a plot of $\delta^{13}C$ against H/C for samples from the three sites, and shows these trends more clearly. Two distinct maturation paths are evident.

Thermal alteration experiments (Ishiwatari et al., 1977; Peters et al., 1981) and analysis of regional metamorphic effects (McKirdy and Powell, 1974; Hoefs and Frey, 1976) have shown that small increases in $\delta^{13}C$ from a few tenths of a per mil to 1.5‰ or more may accompany kerogen maturation into the dry gas zone. Simoneit et al. (1981) found an increase of 2–4‰ in kerogen $\delta^{13}C$ as a result of diabase intrusions in Cretaceous black shales. These increases in $\delta^{13}C$ during kerogen maturation are attributed to the production of isotopically light hydrocarbons by cracking reactions. Whereas the carbon isotope behavior of kerogen from Site 478 is consistent with these findings, the distinct decreases in $\delta^{13}C$ observed at Sites 477 and 481 are not. These results are difficult to explain. Perhaps, again, they are related to differences in sill thickness and time

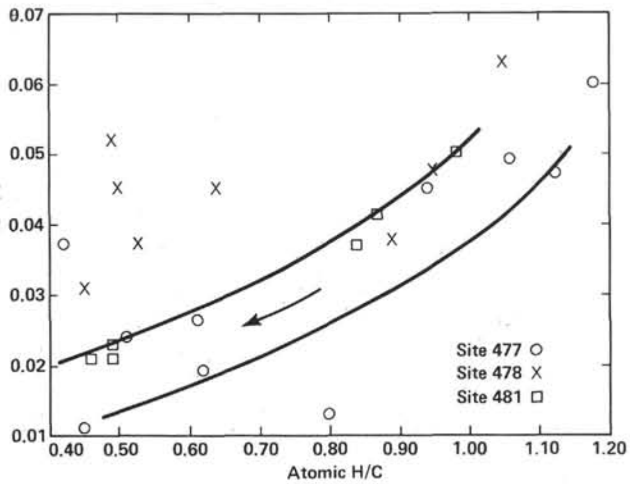

Figure 4. Plot of atomic N/C versus atomic H/C for kerogen samples from Sites 477, 478, and 481. The arrow shows the path of maturation for kerogen from Sites 477 and 481.

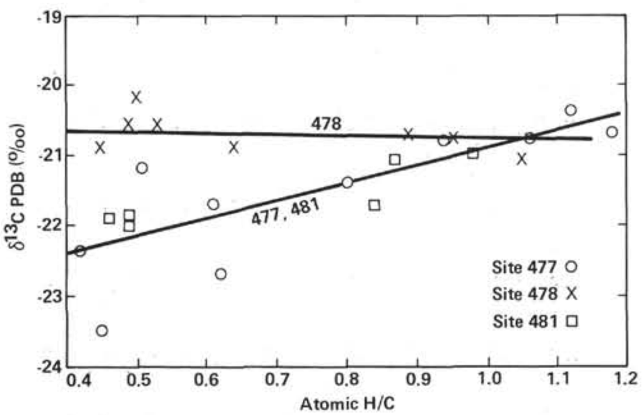

Figure 5. Plot of $\delta^{13}C$ versus atomic H/C for kerogen samples from Sites 477, 478, and 481. Note that the samples from Site 478 appear to describe a different maturation trend than those from Sites 477 and 481.

of heating. The sediments recovered at Sites 477, 478 and 481 are all of Pleistocene age. Very young sedimentary organic matter might be expected to retain a large part of the isotopic heterogeneity present in precursor biota (Abelson and Hoering, 1961; Galimov, 1974). Moreover, young sediments typically contain appreciable amounts of humic and fulvic acids and these are known to be enriched in ^{13}C relative to coexisting protokerogen (Nissenbaum and Kaplan, 1972). Simoneit et al. (1979) found that an average of 20% of the organic carbon in surface sediments of the Guaymas Basin is present as humic acid. In contrast, virtually no humic acid was recovered from the Cretaceous black shales of the Eastern Atlantic (Simoneit et al., 1981). The difference in $\delta^{13}C$ behavior among the Guaymas Basin sites may therefore be due to more complete elimination of some thermally labile, isotopically heavy fraction of the organic matter at Sites 477 and 481 than at Site 478.

Electron Spin Resonance Data

The ESR *g* values of all the samples (with the exception of Section 477-22-1) lie between 2.0027 and 2.0031 (Table 1). There is no apparent change in *g* value with maturity. This is noteworthy because previous studies have reported decreasing *g* value with increasing organic maturity in shales (Pusey, 1973; Ho, 1979; Marchand and Conard, 1980), in sediments intruded by basalt (Baker et al., 1978), and in artificially heated kerogens (Ishiwatari et al., 1977; Marchand and Conard, 1980). The lack of variation in *g* value with maturity may be due to the presence of significant amounts of humic acids in the protokerogen of this study. Ho (1979) has compiled data showing that, on the average, the *g* values of humic acids (2.0021 to 2.0031) are less than those of associated protokerogens (2.0025 to 2.0039). In addition, he found that preliminary extraction of humic acids from Tertiary sediments off the coast of Texas increased the *g* values of isolated organic matter by two or more units in the last decimal place. As the total range of *g* values for marine kerogen during maturation can be quite small (e.g., 4–5 units for the Toarcian of the Paris Basin; Marchand and Conard, 1980), the presence of humic acid could virtually mask any variation with maturity.

Figures 1C–3C show that ESR spin density increases with proximity to the dolerite sills. This is presumably due to the generation of free radicals by homolytic cleavage of alkyl side chains from the protokerogen. As the aromaticity of the protokerogen increases, more and more of these radicals are stabilized by delocalization on aromatic carbon sheets (Austen et al., 1966). The detailed sampling at Site 478 (Figure 2C) shows that very near the sill contact spin density decreases again. Ho (1979) and Ishiwatari et al. (1977) have explained this reversal as a result of electron pairing and the elimination of structural defects during graphitization of the kerogen.

Figure 6 shows a plot of *N* versus H/C for Sites 477, 478, and 479. Some of the variation in spin density at a given H/C value may be due to differing proportions of two or more maceral types in the kerogen (Morishima and Matsubayashi, 1978). Nevertheless, the spin concentrations of kerogens from Site 478 are generally lower than the spin concentrations of kerogens from Site 477 and appear to follow a different maturation path. Immature kerogens at both sites have spin densities of $1\text{–}10 \times 10^{17}$ spins/g C. Kerogens from Sites 477 and 481, however, show a slow initial increase in spin density with increasing maturity followed by a sharp maximum of 200×10^{17} spins/g C at an H/C of 0.45. In contrast, kerogen from Site 478 shows a sharp increase in spin density with increasing maturity followed by a broad maximum of 85×10^{17} spins/g C at an H/C of 0.64. The differences between the spin density behavior at Sites 477 and 481 and that at Site 478 may be due to the different time/temperature regimes imposed by the dolerite sill thickness. Simoneit et al. (1981) observed a spin density maximum of 80×10^{17} spins/g kerogen at

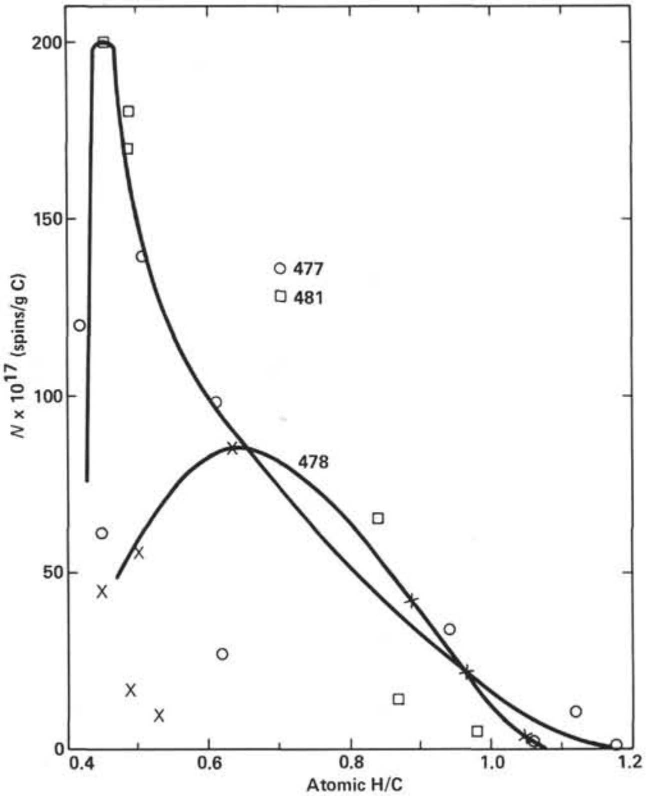

Figure 6. Plot of ESR spin density (N) versus atomic H/C for kerogen samples from Sites 477, 478, and 481. Note that the samples from Site 478 appear to describe a different maturation trend than those from Sites 477 and 481.

an H/C of 0.61 for the altered black shales of the Eastern Atlantic.

Figures 1D–3D show the behavior of line width in the vicinity of the dolerite sills. The data from Figure 2D suggest that, like spin density, line width may pass through a maximum during thermal alteration. A plot of line width versus H/C for all three sites (Fig. 7) supports this possibility. Despite the scatter (some of which may be due to differing proportions of two or more maceral types), line width seems to show a maximum of

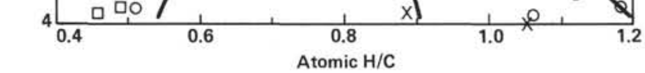

Figure 7. Plot of ESR line width (ΔH) versus H/C for kerogen samples from Sites 477, 478, and 481. The arrow denotes the general path of maturation.

about 6.5 at an H/C of 0.64. The large line width at 7.7 gauss appears to be anomalous, as discussed previously.

Baker et al. (1977) observed a much larger range of line widths for organic matter from the Eastern Atlantic Cretaceous black shales. They found that immature kerogens had line widths of approximately 10 gauss and that these values decreased to as little as 3.3 gauss with severe alteration. The latter value is comparable to the 4 gauss line widths observed for highly altered kerogens in this study. (This is especially true since the 5-gauss magnetic field modulation amplitude used in this study, although providing high signal sensitivity, produced slightly exaggerated line widths.) The difference in ΔH of immature kerogens between this study (4 gauss) and that of Baker et al. (10 gauss) could be due to procedural differences, since Baker et al. did not extract their kerogens with organic solvents before running spectra. Alternatively, the discrepancy in immature kerogen line width could be due to compositional (source) differences or perhaps to the older, diagenetically more mature nature of the Cretaceous samples. The data of Baker et al. (1977) are thus not necessarily inconsistent with the results of the present study.

There is a strong urge to relate ESR line width behavior to some physico-chemical aspect of kerogen maturation. As mentioned before, the maximum in ESR spin density during kerogen maturation is generally thought to reflect the production of free radicals as hydrocarbons are cracked from the kerogen structure. Decreasing g values during kerogen maturation have been related to the loss of oxygen-containing functional groups (Ishiwatari et al., 1977; Marchand and Conard, 1980). It is difficult, however, to explain ESR line width in a similar fashion, at least in part because of the widely differing maturation behaviors reported in the literature. Some authors have shown increases in line width with kerogen maturity (Pusey, 1973; Ishiwatari et al., 1977). Other authors have reported decreases (Ho, 1979; Baker et al., 1977). Still others have observed an increase in line width followed by a maximum and a decrease (Peters, 1978; Morishima and Matsubayashi, 1978; this chapter). It seems apparent that before meaningful progress can be made in understanding ESR line width as a function of kerogen maturity, uniform procedures for isolating, characterizing, and scanning kerogens must be established among laboratories.

CONCLUSIONS

Significant thermal alteration of protokerogen at Sites 477, 478, and 481 has occurred as a result of the intrusion of dolerite sills. Kerogen atomic H/C values as low as 0.4 are observed in the vicinity of the sills. During alteration, ESR line width passes through a maximum 6.5 gauss at an approximate H/C of 0.64. ESR g value, on the other hand, shows no correlation with maturity, perhaps owing to the presence of humic acids in the samples.

Atomic N/C, carbon isotope composition, and ESR spin density all demonstrate the effects of thermal stress near the sill contacts. Their behavior, however, is not uniform among the three sites. At Sites 477 and 481, N/C values decrease sharply near the sills to values of 0.025 and less. In contrast, N/C values near the small sill at Site 478 remain as high as 0.05. $\delta^{13}C$ decreases by 1 to 1.5‰ in the sill vicinities at Sites 477 and 481, whereas it increases slightly at Site 478. Finally, spin density shows a more intense maximum at Sites 477 and 481 than at Site 478 and the maximum occurs at a lower H/C value. These incongruities do not seem likely to be a result of compositional differences but may instead reflect differences in sill thickness (and hence intensity and duration of thermal stress) at the three sites. It is proposed that some thermally sensitive, isotopically heavy, and perhaps nitrogen-rich component of the Guaymas Basin protokerogen has been more completely destroyed at Sites 477 and 481 than at site 478. The chemical and isotopic heterogeneity of recently deposited protokerogen may thus cause a more complex response to thermal stress than would normally be expected of a kerogen which has already undergone an extensive period of low-temperature diagenetic alteration.

ACKNOWLEDGMENTS

We thank Mr. D. Winter for stable isotope determinations and gratefully acknowledge partial financial assistance from the National Aeronautics and Space Administration (Grant No. NGR 05-007-221). We thank K. E. Peters and H. I. Halpern for reviews of this manuscript. Contribution No. 2191 from the Institute of Geophysics and Planetary Physics, University of California at Los Angeles.

REFERENCES

Abelson, P. H., and Hoering, T. C., 1961. Carbon isotope fractionation in formation of amino acids by photosynthetic organisms. *Proc. Nat. Acad. Sci.*, 47:623-632.

Austen, D. E. G., Ingram, D. J. E., Given, P. H., Binder, C. R., and Hill, L. W., 1966. Electron spin resonance study of pure macerals. *In* Given, P. H. (Ed.), *Coal Science:* Advanc. Chem. Ser. No. 55: Washington (American Chemical Society), 344-362.

Baker, E. W., Huang, W. Y., Rankin, J. G., Castaño, J. R., Guinn, J. R., and Fuex, A. N., 1978. Electron paramagnetic resonance study of thermal alteration of kerogen in deep-sea sediments by basaltic sill intrusion. *In* Lancelot, Y., Seibold, A., et al., *Init. Repts. DSDP,* 41: Washington (U.S. Govt. Printing Office), 839-847.

Curray, J. R., Moore, D. G., and the Shipboard Scientific Party, 1979. Deep Sea Drilling Project in the Gulf of California, Leg 64. *Geotimes*, 24(7):18-20.

Degens, E. T., 1969. Biogeochemistry of stable carbon isotopes. *In* Eglinton, G., and Murphy, M. T. J. (Eds.), *Organic Geochemistry:* New York (Springer-Verlag), pp. 304-329.

Durand, B., and Monin, J. C., 1980. Elemental analysis of kerogens (C, H, O, N, S, Fe). *In* Durand, B. (Ed.), *Kerogen:* Paris (Editions Technip), pp. 113-142.

Frazer, J. W., 1962. Simultaneous determination of carbon, hydrogen and nitrogen. Part II. *Mikrochim. Acta*, 993-999.

Galimov, E. M., 1974. Organic geochemistry of carbon isotopes. *In* Tissot, B., and Bienner, F. (Eds.), *Advances in Organic Geochemistry 1973:* Paris, (Editions Technip), pp. 439-452.

Ho, T. T. Y., 1979. Geological and geochemical factors controlling electron spin resonance signals in kerogen. *UNESCAP/CCOP Tech. Publ.* 6:54-80.

Hoefs, J., and Frey, M., 1976. The isotopic composition of carbonaceous matter in a metamorphic profile from the Swiss Alps. *Geochim. Cosmochim. Acta*, 40:945-951.

Ishiwatari, R., Ishiwatari, M., Rohrback, B. G., and Kaplan, I. R., 1977. Thermal alteration experiments on organic matter from recent marine sediments in relation to petroleum genesis. *Geochim. Cosmochim. Acta*, 41:815-828.

McKirdy, D. M., and Powell, T. G., 1974. Metamorphic alteration of carbon isotopic composition in ancient sedimentary organic matter: New evidence from Australia and South Africa. *Geology*, 2:591-595.

Marchand, A., and Conard, J., 1980. Electron paramagnetic resonance in kerogen studies. *In* Durand, B. (Ed.), *Kerogen:* Paris (Editions Technip), pp. 243-270.

Morishima, H., and Matsubayashi, H., 1978. ESR diagram: A method to distinguish vitrinite macerals. *Geochim. Cosmochim. Acta*, 42:537-540.

Nissenbaum, A., and Kaplan, I. R., 1972. Chemical and isotopic evidence for the *in situ* origin of marine humic substances. *Limnol. Oceanogr.*, 17:570-582.

Peters, K. E., 1978. Effects on sapropelic and humic protokerogen during laboratory-simulated geothermal maturation experiments [Ph.D. Dissert.]. University of California, Los Angeles.

Peters, K. E., Rohrback, B. G., and Kaplan, I. R., 1981. Carbon and hydrogen stable isotope variations in kerogen during laboratory-simulated thermal maturation. *Am. Assoc. Pet. Geol. Bull.*, 65: 501-508.

Peters, K. E., Simoneit, B. R. T., Brenner, S., and Kaplan, I. R., 1974. Vitrinite reflectance-temperature determinations for intruded Cretaceous black shale in the Eastern Atlantic. *In* Oltz, D. F. (Ed.), *Symp. Low Temp. Metamorphism Kerogen Clay Miner.:* Los Angeles (Pac. Sect., Soc. Econ. Paleontol. Mineral.), pp. 53-58.

Pusey, W. C., 1973. Paleotemperatures in the Gulf Coast using the ESR-kerogen method. *Trans. Gulf Coast Assoc. Geol. Sci.*, 23: 195-212.

Simoneit, B. R. T., Brenner, S., Peters, K. E., and Kaplan, I. R., 1981. Thermal alteration of Cretaceous black shale by diabase intrusions in the Eastern Atlantic: II. Effects on bitumen and kerogen, *Geochim. Cosmochim. Acta.*, 45:1581-1602.

Simoneit, B. R. T., Mazurek, M. A., Brenner, S., Crisp, P. T., and Kaplan, I. R., 1979. Organic geochemistry of recent sediments from Guaymas Basin, Gulf of California. *Deep Sea Res.*, 26A:879-891.

Stuermer, D. H., Peters, K. E., and Kaplan, I. R., 1978. Source indicators of humic substances and protokerogen. Stable isotope ratios, elemental compositions and electron-spin resonance spectra. *Geochim. Cosmochim. Acta*, 42:989-977.

Waples, D. W., 1977. C/N ratios in source rock studies. *Min. Ind. Bull.*, 20(5):1-7.

Welte, D. H., Hagemann, H. W., Hollerbach, A., Leythaeuser, D., and Stahl, W., 1975. Correlation between petroleum and source rock. *Proc. 9th World Pet. Cong.*, 2:179-191.